Direct and Reverse Mechanical Modeling of an Alkyd Acrylic Hybrid System: A Morphological Study

Didier Colombini, Mehrnoush Jowkar-Deriss, Ola J. Karlsson, and Frans H. J. Maurer*

Department of Polymer Science & Engineering, Lund University, Lund Institute of Technology, Box 124, SE-22100 Lund, Sweden

Received July 21, 2003; Revised Manuscript Received December 5, 2003

ABSTRACT: Mechanical modeling and dynamic mechanical analysis were associated to investigate the viscoelastic properties of an alkyd acrylic hybrid system in connection with its morphology, which was characterized by transmission electron microscopy. Theoretical predictions based on the interlayer model used in direct mode were successfully combined with the experimental viscoelastic data to lead to relevant additional information about the complex particulate morphology of the hybrid system. Thus, using direct mechanical modeling, it was concluded that the experimental response of the alkyd acrylic hybrid system to a sinusoidal mechanical stress corresponds to the mechanical response of a sample whose morphology involves a acrylic-rich interphase between continuous and dispersed alkyd-rich domains. For the very first time, the interlayer model was then used in reverse mode in order to separate the actual viscoelastic properties of such a acrylic-rich interphase from those experimentally obtained for the alkyd acrylic hybrid system. The differences in these extracted viscoelastic properties, when compared to those of the pure latex film, were presented as reflecting the changes in the molecular mobility of the macromolecules resulting from the mutual influence of the phases in the multiphase hybrid material.

1. Introduction

In the past several decades, the growing environmental awareness has led to an increasing interest in the replacement of solvent-borne surface coatings with their aqueous-based counterparts, i.e., environmentally friendly waterborne systems. Among the different types of waterborne binders existing in today's market are acrylic latex dispersions and alkyd emulsions, both having their own characteristic advantages and disadvantages. Thus, the acrylic latex coatings show, for example, short drying time, low odor, and easy cleanup with water, but their penetration in the substrate is inferior to that of alkyd emulsions. On the other hand, alkyd emulsions typically have high gloss and good penetration but show much longer drying times than the acrylic latex dispersions. A new research area investigating hybrid systems consisting of both latex dispersions and alkyd emulsions has logically arisen[1−12] from the expectation that the association of both types of waterborne binders could diminish their negative contribution in the final systems. In this way, alkyd acrylic hybrid systems would therefore potentially combine the fast drying and the color retention of the acrylic latexes with the high gloss and the good penetration properties of the alkyd emulsions.

The present study focuses on such an alkyd acrylic hybrid system, whose viscoelastic properties were aimed to be investigated in connection with its morphology. In addition, this works mainly concerns the use and optimalization of mechanical modeling and dynamic mechanical analysis as tools for extracting relevant morphological information in multipolymeric materials.

2. Sample Preparation and Characterization

2.1. Materials and Sample Preparation. 2.1.1. Materials. In the present paper, we briefly describe the chemicals and pure constituents as well as the preparation of the investigated alkyd acrylic hybrid system, for which an extended description that includes more details has previously been given.[13−15]

The used linseed oil alkyd, liquid at room temperature (viscosity $\eta = 1.3$ Pa s at 23 °C, 100 s^{-1}), was supplied by Akzo Nobel Decorative Coatings AB, Sweden. The siccative (drier, also supplied by Akzo Nobel Decorative Coatings AB, Sweden), containing 6% Co and 9% Zr, was added (as supplied) to the alkyd, at 0.05 wt % Co based on the alkyd weight, and mixed.

The acrylate dispersion was supplied by Celanese Emulsions Norden AB, Sweden, having a glass transition temperature around 60 °C, a solids content of 56 wt %, and a particle size around 300 nm.

The hybrid system was prepared by charging the latex dispersion into a 1 L glass reactor immersed in a thermostated water bath with a temperature of 50 °C. The alkyd/siccative mixture was first separately heated to 50 °C and slowly added (∼3−4 g min^{-1}) under stirring (∼400 rpm) to the reactor containing the latex dispersion. For the stabilization of the alkyd droplets in the hybrid, a solution (2.6 M) of sodium hydroxide (NaOH, supplied by Merck, Germany) was added to the latex dispersion prior to the addition of the alkyd/siccative mixture to give a final pH value of 7−8 in the hybrid.[13−15] The final alkyd/acrylate solid weight ratio in the hybrid system was 67/33.

2.1.2. Film Formation. The hybrid films were prepared by applying the hybrid mixture onto clean glass plates, with an applicator bar leading to a wet film thickness of 0.2 mm. The films were then left to dry at ambient temperature and relative humidity for 7 days. This procedure was repeated until the final dry thickness of the hybrid films had reached 0.8 mm. Subsequently, the films were further dried in a vacuum oven for 2 days at 40 °C, and they were then kept in a desiccator at ambient temperature.

In addition, some films based on the pure constituents were also prepared. Thus, a latex film was formed in a conventional oven at 65 °C, and a film based on the alkyd emulsion (with an amount of NaOH leading to a same pH value as in the hybrid system) was prepared by following the procedure above described for the hybrid films.

2.2. Sample Characterization. 2.2.1. Dynamic Mechanical Analysis (DMA). The TA Instruments "dynamic mechanical analyzer" DMA 2980 was used operating in tensile mode

* Corresponding author: e-mail frans.maurer@polymer.lth.se; phone +46 46 222 91 49; fax +46 46 222 41 15.

10.1021/ma030395h CCC: $27.50
Published on Web 03/02/2004

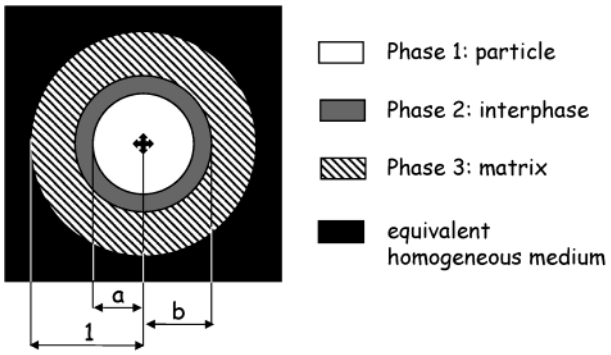

Figure 1. Illustration of a representative volume element (RVE) of the interlayer model.

under isochronal conditions at the frequency of 1 Hz to measure the temperature dependence of the absolute value of the complex elastic modulus $|E^*|$ (storage, E', and loss, E'', moduli) and loss factor tan δ of the films (latex, alkyd, and hybrid).

The samples were approximately 18 mm long, 5 mm wide, and 0.8 mm thick. The viscoelastic spectra were recorded from −60 to 120 °C with a heating rate of 3 °C/min.

2.2.2. Transmission Electron Microscopy (TEM). The morphology of the hybrid film was examined by TEM using a Philips CM10 transmission electron microscope. First, the sample was cut in ultrathin sections, having a thickness around 70 nm, in an ultramicrotome using a diamond knife. Positive staining of the sections was then carried out with osmium tetroxide (OsO_4), which reacted with residual double bonds in the alkyd phase of the hybrid for 50 min. In the TEM micrographs, the alkyd-rich phase appears as dark domains and the acrylic acrylic-rich phase as bright domains.

3. Mechanical Modeling−Self-Consistent Schemes

3.1. Presentation. The prediction of the complex moduli of multiphase polymeric materials, including polymer blends and composite materials, is usually based on phenomenological laws,[16−18] variational methods,[19−21] or self-consistent schemes[22−28] extended to describe viscoelastic behavior[29−40] through the correspondence principle.[41]

The interlayer model[28,42] used in this work represents an extension of van der Poel's theory,[43] which is closely connected to previous work[44] on the description of the viscosity of suspensions by a shell model. In comparison with the other theoretical approaches,[16−18] it is here important to point out that mechanical models based on self-consistent schemes (i.e., such as the interlayer model) do not include any adjustable parameters. To predict the dynamic mechanical shear properties of multipolymeric materials, the interlayer model requires the definition of a representative volume element (RVE). Such an RVE, depicted in Figure 1, basically consists of three concentric spheres embedded in an equivalent homogeneous medium: the matrix (phase 3) covers a shell of interphase (phase 2), surrounding the particle (phase 1). The radii of the concentric spheres are chosen in accordance with the volume fractions of the different phases. In this way, $V_1 = a^3$, $V_2 = b^3 - a^3$, and $V_3 = 1 - b^3$. Such a geometrical arrangement that is independent of the dispersed particle size is therefore representative of both the morphology and the composition of the investigated multicomponent material.

Calculations are based on a set of common assumptions, which are (i) linear elastic and viscoelastic behavior of phases, (ii) homogeneous and isotropic phases, (iii) continuity of displacements and radial and tangential stresses at the boundaries of the phases, and (iv) no inertial forces, no defects, and no thermal stresses. On the basis of these boundary conditions, it is assumed that the response of the RVE to an external shear stress field is equal to the response of a volume element of homogeneous multipolymeric material. The entire description of the equations involved in the interlayer model has been reported earlier.[30,40,42]

3.2. Direct and Reverse Mechanical Modeling. The use of self-consistent mechanical models in direct and reverse modes has been shown[29,30,33−40,42] to be of great interest for giving an in-depth description and discussion of the possibilities and limitations of the theoretical mechanical approach in the understanding of dynamic mechanical data of complex multiphase polymeric materials.

Direct mechanical modeling is the usual mode of use.[29,30,33,35,36,38−40,42] As illustrated in Figure 2a, it leads to the prediction of the viscoelastic properties of a multiphase material from the knowledge of the viscoelastic properties of all pure constituents: the composition as well as the morphology of the material is also required for numerical simulations. Thus, direct mechanical modeling permits to highlight the mechanical coupling effects between phases in connection with morphology. In that respect, it was found[35,36,39,45] that the magnitude of these effects between phases depends not only on mechanical properties and relative content of each phase but also on the geometric arrangement of the phases. In addition, since several morphologies can be taken into account in the calculation, the theoretical predictions were also presented[29,35,36] as an interesting qualitative probe of the morphology of multicomponent materials.

The reverse mode was recently proposed[34,36,37] and permits (see Figure 2b) the extraction of the actual viscoelastic characteristics of one phase blended among others in a heterogeneous polymeric system for specific morphologies. In reverse mechanical modeling, the experimental viscoelastic properties of the multiphase material are used as input data in association with the blend composition and the viscoelastic properties of the pure constituents. Such a new approach for mechanical modeling was shown[36,37] to be of particular interest for investigating the actual viscoelastic properties of the interfacial area in multiphase polymeric materials, whose experimental in-situ detection and characterization remain problematic.

4. Results and Discussion

4.1. Experimental Section. 4.1.1.Viscoelastic Properties: DMA. The viscoelastic properties of the pure constituents as well as those of the alkyd acrylic hybrid are given in Figure 3. It can be seen that the α-relaxations associated with the glass transitions of the pure alkyd emulsion and latex films lead to maxima of the loss factor tan δ at 20 °C (maximum of the loss modulus $E''_{\text{alkyd emulsion}}$ at 3 °C) and at 82 °C (maximum of the loss modulus E''_{latex} at 64 °C), respectively.

In the mechanical thermogram of the hybrid system, no significant change in the viscoelastic characteristics of the alkyd-rich phase are observed, when compared to those of the pure alkyd emulsion film. On the other hand, the temperature location of the maxima associated with the glass transition of the acrylic-rich phase in the alkyd acrylic hybrid is slightly shifted toward lower temperatures.

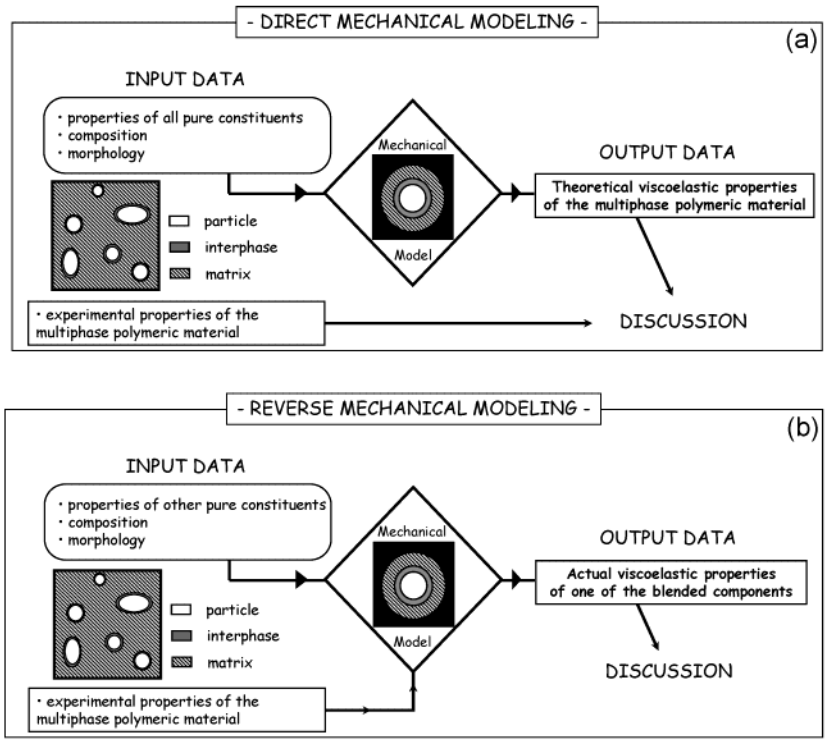

Figure 2. Schematic illustration of the two modes of use of mechanical models: (a, top) direct mode; (b, bottom) reverse mode.

4.1.2. Morphology: TEM. Figure 4 shows the TEM micrograph of OsO_4-stained hybrid film where the acrylic-rich phase appears as bright domains and the alkyd-rich phase as dark domains.

What can be seen on the picture is a rather complex particulate morphology, which can be discussed in several ways, at different observation scales. Although the distinction between the acrylic-rich phase and the alkyd-rich phase is perfectly clear (Figure 4), the morphology of the alkyd acrylic hybrid system cannot be undoubtedly described. As a matter of fact, at least four different particulate morphologies can be supported by the TEM micrograph. As illustrated in Figure 5, the acrylic-rich phase in the alkyd acrylic hybrid system can be considered either as a matrix (Figure 5a), as a particle (Figure 5b), or as an interphase (Figure 5d), and vice versa for the alkyd-rich phase, considered as dispersed (Figure 5a), continuous (Figure 5b) or as interphase (Figure 5c).

4.2. Theoretical Section. Since the interlayer model can predict the mechanical viscoelastic properties of particulate multicomponent polymeric materials in relation to their morphology, can such a theoretical approach be helpful for the description of the morphology (Figure 4) with respect to the viscoelastic properties (Figure 3) of the alkyd acrylic hybrid system?

4.2.1. Direct Mode. On the basis of the definition of an RVE, not only three-phase "particle−interphase−matrix" RVE are available for calculation. As a matter of fact, from a theoretical point of view, it is easy to perform numerical simulations by assuming a volume fraction of interphase equal to zero, therefore corresponding to a two-phase particulate system (i.e., represented by a two-phase RVE). As a consequence, the four particulate morphologies presented in Figure 5 can be theoretically investigated by direct mechanical modeling, using either a two-phase RVE or a three-phase RVE. Insofar as the composition of the hybrid system, i.e., A67:L33 (alkyd emulsion:latex, weight part ratio), and the viscoelastic properties of its pure constituents (Figure 3) are known, only the geometrical arrangement of the phases in the RVE does change in all of the following numerical simulations.

a. Calculation Using a Two-Phase RVE. Two distinct geometrical arrangements are available and representative of a particulate morphology where the latex phase acts either as the continuous phase (as illustrated in Figure 5a) or as the dispersed phase (as illustrated in Figure 5b). In the present paper, the results of the corresponding "particle−matrix" numerical simulations are denoted A67/L33 (Figure 5a) and L33/A67 (Figure 5b), respectively.

b. Calculation Using a Three-Phase RVE. Two distinct geometrical arrangements are available and representative of a particulate morphology including an interphase based either on the alkyd emulsion (as illustrated in Figure 5c) or on the latex (as illustrated in Figure 5d). However, since the particle (i.e., phase 1 in Figure 1) and the matrix (i.e., phase 3 in Figure 1) are based on the same constituent (either the latex or the alkyd emulsion, respectively) in the RVE, several "particle−interphase−matrix" phase repartitions are possible in the numerical simulations. In the present paper, they are denoted A(67−m)/L33/A(m) and L(33−n)/A67/L(n), with $m < 67$ and $n < 33$ defined as the fraction of alkyd emulsion or latex which is considered as continuous phase in the simulations, respectively. In concrete terms, only calculations considering values of m equal to 27, 40, or 57 and values of n equal to 5, 13, or 28 are presented in this study (even if many other values of m and n also were investigated).

The theoretical predictions of the viscoelastic data of the alkyd acrylic hybrid system, involving either a two-phase RVE or a three-phase RVE, are plotted in Figure 6 and Figure 7, respectively. For a clearer overview and to make the comparison easier, the experimental viscoelastic properties of the hybrid system are also included in these figures.

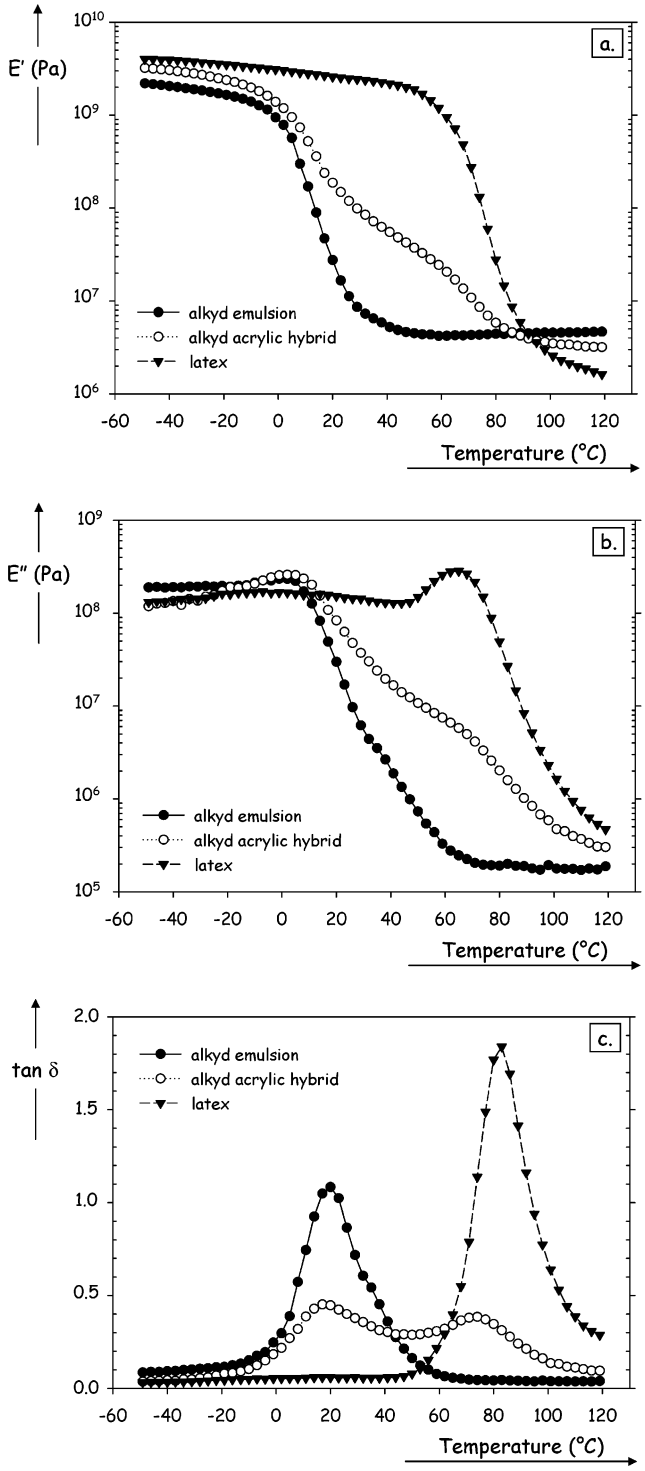

Figure 3. Viscoelastic properties of the pure constituents and the alkyd acrylic hybrid: (a) storage modulus (E') vs temperature; (b) loss modulus (E'') vs temperature; (c) loss factor (tan δ) vs temperature.

Significant differences between the predictions can be noticed already in Figure 6, depending on which morphology was taken into account in the two-phase RVE (at a constant composition). However, none of these predictions involving a two-phase particulate morphology (Figure 6) successfully describe the experimental viscoelastic behavior of the hybrid system. The situation is significantly improved in Figure 7, where some of the predictions are found close to the experimental data, when compared to those given in Figure 6. Both predictions denoted L28/A67/L5 and A27/L33/A40 lead to the

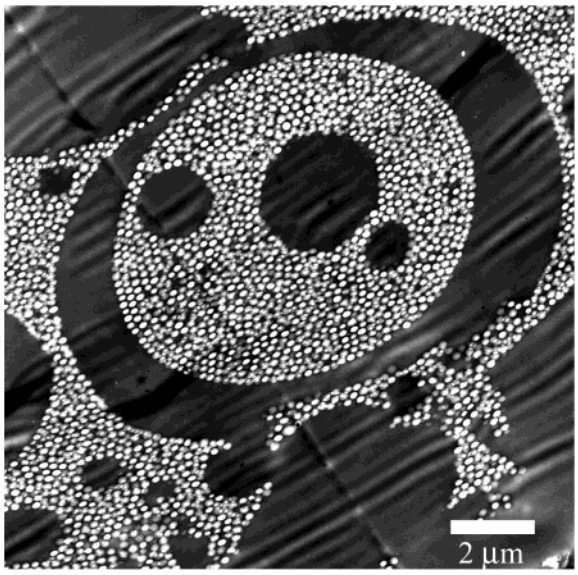

Figure 4. TEM micrograph of the alkyd acrylic hybrid.

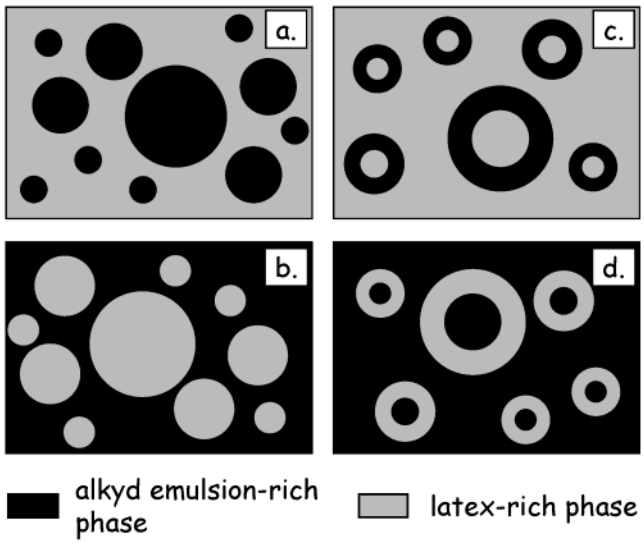

Figure 5. Schematic representation of the different particulate morphologies supported by the TEM micrograph.

best fits with the experimental data. However, according to the TEM micrograph (Figure 4), the phase repartition in the three-phase RVE involving an alkyd-rich interphase (i.e., L28/A67/L5) cannot be considered as realistic since only five parts of the latex would then be devoted to the continuous phase. On the other hand, the phase repartition A27/L33/A40 appears well acceptable: this may therefore suggest that the TEM micrograph can be described as containing a acrylic-rich interphase between dispersed and continuous alkyd-rich phases.

A complementary association of both experimental and theoretical viscoelastic data can be obtained by plotting the relative energy dissipation per cycle against the dynamic tensile modulus E_d (defined as $E_d^2 = E'^2 + E''^2$). The relative energy dissipation was given[35,36] by the ratio of the dissipated energy (ΔW) and the total energy (W) on a cycle of dynamic mechanical strain. Precisely, $\Delta W/W$ can be expressed as a function of the loss factor tan δ (i.e., E''/E'), as follows:

$$\frac{\Delta W}{W} = 2\pi \frac{\tan \delta}{\sqrt{(1 + \tan^2 \delta)}}$$

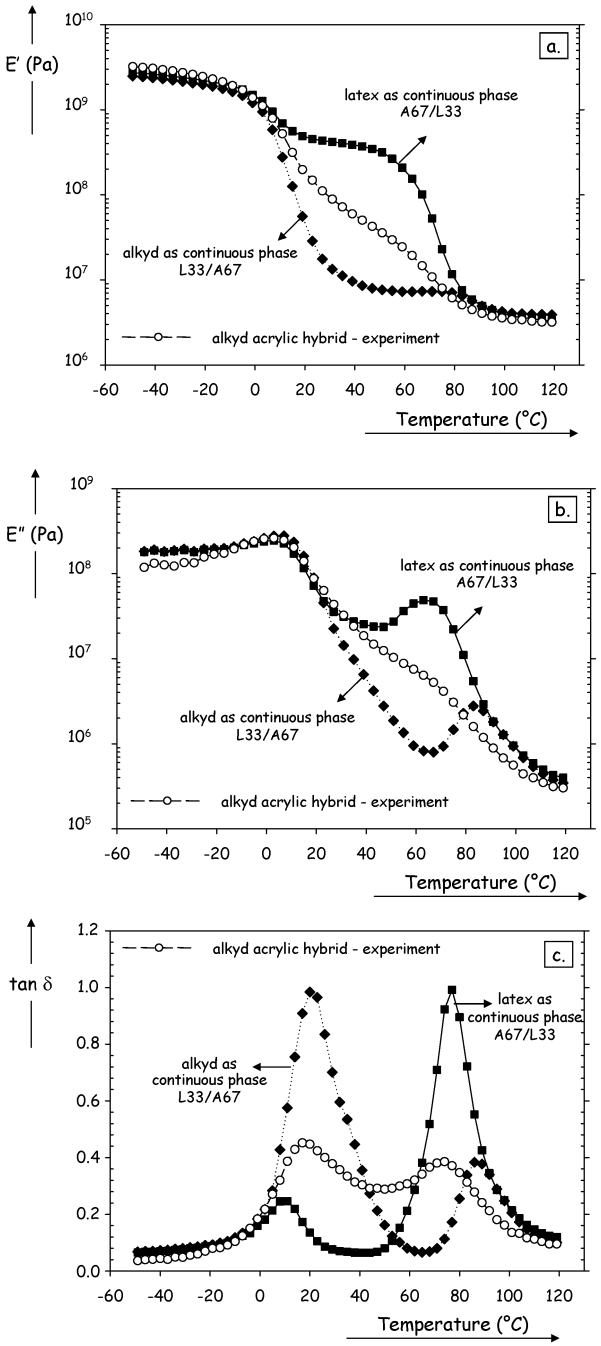

Figure 6. Theoretical predictions of the viscoelastic properties of the hybrid system as a function of the morphology taken into consideration (two-phase RVE): (a) storage modulus (E') vs temperature; (b) loss modulus (E'') vs temperature; (c) loss factor (tan δ) vs temperature. The experimental viscoelastic properties of the alkyd acrylic hybrid are recalled for comparison.

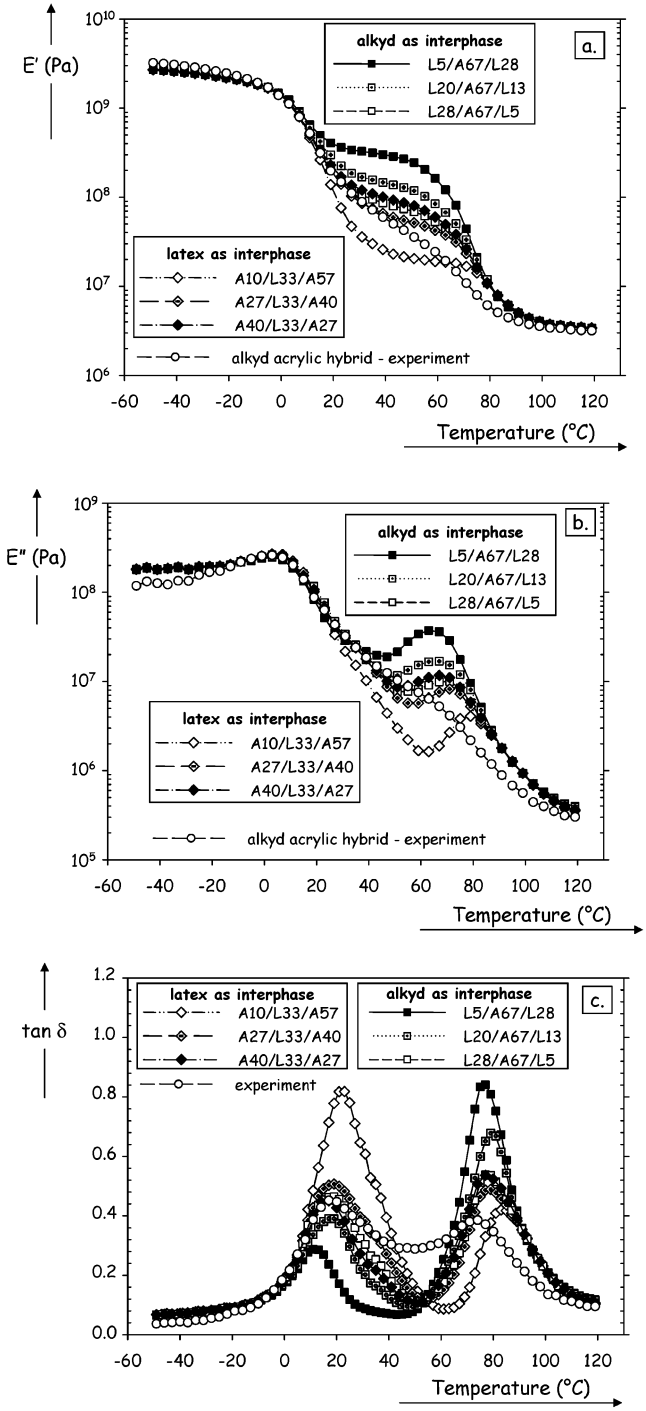

Figure 7. Theoretical predictions of the viscoelastic properties of the hybrid system as a function of the morphology taken into consideration (three-phase RVE): (a) storage modulus (E') vs temperature; (b) loss modulus (E'') vs temperature; (c) loss factor (tan δ) vs temperature. The experimental viscoelastic properties of the alkyd acrylic hybrid are recalled for comparison.

Such a representation of the viscoelastic data is of particular interest since both axes are functions of the storage (E') and the loss (E'') moduli of the material, and therefore neither the temperature dependence nor the frequency dependence appears directly. Since the morphology of the multicomponent materials is taken into account through the definition of the geometrical arrangement of the spheres in the RVE, the comparison between both experimental and theoretical plots was presented[35,36] as an interesting qualitative probe of the morphology of multipolymeric systems. In Figure 8, the experimental evolution of $\Delta W/W$ vs E_d for the alkyd acrylic hybrid system is compared to those theoretically obtained by using the interlayer model. For clarity reasons, only the best fits (Figure 7) obtained with the three-phase RVE are associated with the ones resulting from the two-phase RVE (i.e., A67/L33 and L33/A67). Figure 8 significantly points out the differences between all the predictions, which only differ by the geometrical arrangement of their phases. It also becomes clear that the prediction denoted A27/L33/A40 correlates well with the experimental data. In other terms, it can be con-

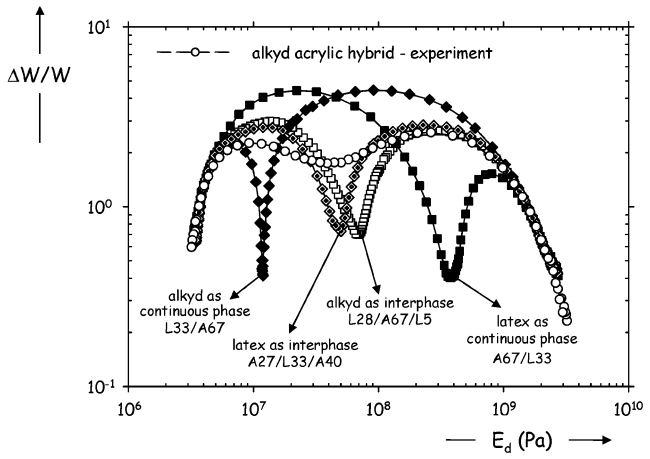

Figure 8. Relative energy dissipation ($\Delta W/W$) vs dynamic tensile modulus (E_d). Theoretical predictions (best curves from two- and three-phase RVE) and experimental viscoelastic properties of the alkyd acrylic hybrid.

cluded that, in agreement with experimental DMA and TEM results, both supported by the theoretical predictions based on the interlayer model used in direct mode, the alkyd acrylic hybrid system can be undoubtedly considered as containing a acrylic-rich interphase between continuous and dispersed alkyd-rich domains.

4.2.2. Reverse Mode. On one hand, the experimental viscoelastic thermograms (Figure 3) have shown that the mechanical properties of the acrylic-rich phase in the hybrid system are affected by the presence of the alkyd-rich phase. In addition, no significant changes in the viscoelastic behavior of the alkyd-rich phase are observed in the experimental mechanical spectra of the alkyd acrylic hybrid.

On the other hand, the theoretical predictions using the interlayer model in direct mode have pointed out (Figures 6−8) that the experimental response of the hybrid system to a sinusoidal mechanical stress corresponds to the mechanical response of a sample whose morphology involves a acrylic-rich interphase between continuous and dispersed alkyd-rich domains.

Therefore, it may now be of interest to use the interlayer model in reverse mode to extract the actual viscoelastic behavior of the acrylic-rich interfacial area in the alkyd acrylic hybrid system. As a matter of fact, the study of the interphases in multipolymeric materials is of relevant interest, since it is well-known that the interfacial properties strongly affect those of such multiphase samples. Although it seems obvious that the actual properties of interfacial macromolecules differ from those of the pure constituents, their in-situ detection (therefore their characterization) remains a problem. This can be solved by reverse mechanical modeling.

The extracted theoretical predictions of the actual viscoelastic properties of the acrylic-rich interphase in the alkyd acrylic hybrid system are plotted in Figure 9. The numerical reverse calculations were performed considering the A27/L33/A40 phase repartition, i.e., the phase repartition leading to the best fit between the experimental data and the theoretical results obtained by direct mechanical modeling (Figures 6−8).

The comparison between these extracted properties and those experimentally obtained for the pure latex film leads to the observation of significant differences (Figure 9). Although the extracted glassy and rubbery storage moduli of the acrylic-rich interphase are both

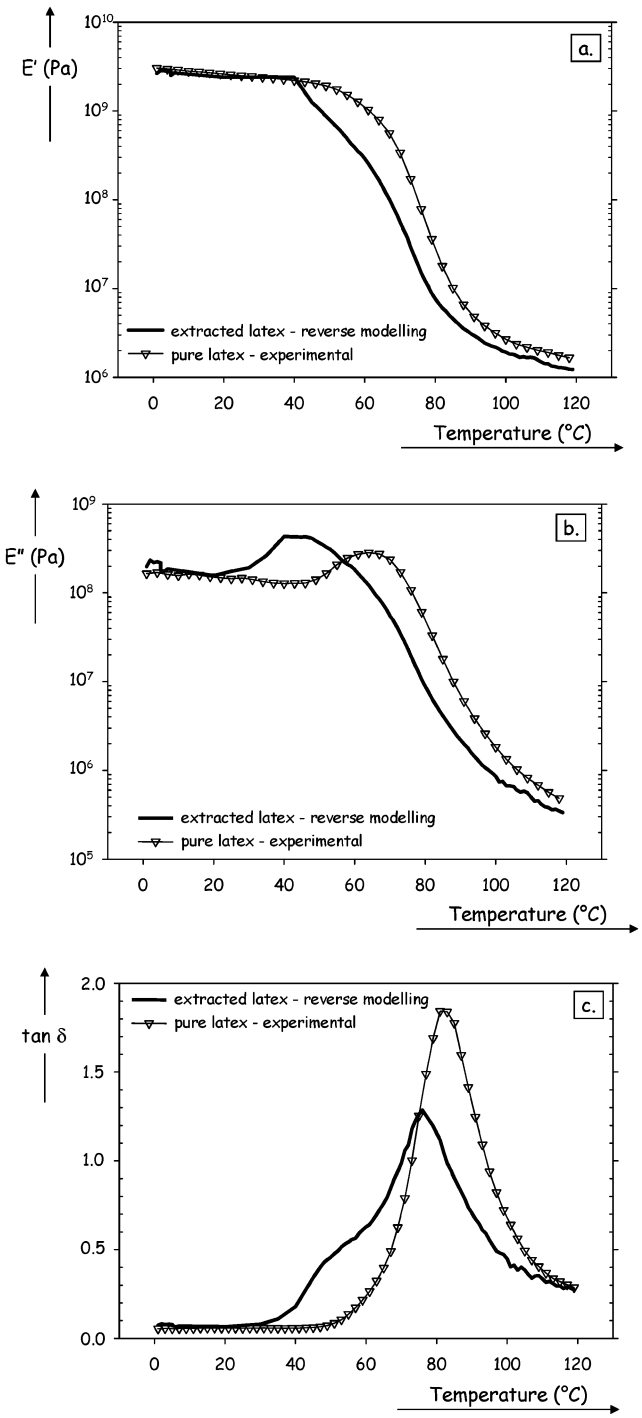

Figure 9. Theoretical predictions of the actual viscoelastic properties of the acrylic-rich interphase in the hybrid system: (a) storage modulus (E') vs temperature; (b) loss modulus (E'') vs temperature; (c) loss factor (tan δ) vs temperature. The viscoelastic properties of the pure latex film are recalled for comparison.

found in the same order than those of the pure constituent (Figure 9a), the modulus drop associated with the glass transition of the latex occurs at significantly lower temperatures in the extracted viscoelastic spectrum. A similar shift toward the lower temperatures is logically also noticed in the temperature location of the corresponding maximum of the extracted loss modulus (E'', Figure 9b). Even if one has to keep in mind that the extracted properties of the latex phase are related to the latex particles (see Figure 4) whereas those of the pure constituent were obtained from a latex film, such

an observation reflects the changes in the molecular mobility of the macromolecules resulting from the mutual influence of both alkyd and latex phases in the hybrid system. Similarly, the observation of a double peak in the extracted loss factor spectra (tan δ, Figure 9c) may also be interpreted as changes in the molecular mobility of the latex macromolecules when blended in the hybrid system.

5. Conclusion

In this study, the interlayer model was used in direct and reverse modes to investigate the viscoelastic properties of an alkyd acrylic hybrid system in connection with its morphology.

The experimental characterization of the hybrid system was performed by transmission electron microscopy (morphology) and by dynamic mechanical analysis (viscoelastic properties). By accounting for various distinct geometrical arrangements of the polymeric phases in direct mechanical modeling (involving either a two-phase RVE or a three-phase RVE), it was found that the complex particulate morphology of the alkyd acrylic hybrid system can be described as containing a acrylic-rich interphase between continuous and dispersed alkyd-rich domains. Thus, direct mechanical modeling (interlayer model) and dynamic mechanical analysis were here successfully associated and led together to additional qualitative information about the morphology of such a multiphase polymeric material, making the full interpretation of its TEM micrograph easier.

For the very first time, the interlayer model was then used in reverse mode in order to investigate the actual viscoelastic properties of the acrylic-rich interphase in the alkyd acrylic hybrid system. The differences in these extracted properties, when compared to those of the pure latex film, were interpreted as a result of the changes in molecular mobility of the macromolecules because of the mutual influence of both alkyd emulsion and latex phases when blended in the alkyd acrylic hybrid material.

Acknowledgment. The authors thank Helen Hassander for transmission electron microscopy works. We gratefully acknowledge the financial support by "The Research school for industry: The Building and its Indoor Environment" organized by "The foundation for knowledge- and competence development (KK-foundation)" and Celanese Emulsions Norden AB, Perstorp, Sweden, and Akzo Nobel Decorative Coatings AB, Malmö, Sweden.

References and Notes

(1) Wu, X. Q.; Schork, F. J.; Gooch, J. W. *J. Polym. Sci., Part A: Polym. Chem.* **1999**, *37*, 4159.
(2) Wang, S. T.; Schork, F. J.; Poehlein, G. W.; Gooch, J. W. *J. Appl. Polym. Sci.* **1996**, *60*, 2069.
(3) Van Hamersveld, E. M. S.; Van Es, J. J. G. S.; German, A. L.; Cuperus, F. P.; Weissenborn, P.; Hellgren, A. C. *Prog. Org. Coat.* **1999**, *35*, 235.
(4) Tsavalas, J. G.; Gooch, J. W.; Schork, F. J. *J. Appl. Polym. Sci.* **2000**, *75*, 916.
(5) Rassing, J.; Boren, M.; Ryrfors, L.-O.; Jönsson, J.-E. Ep 0874875, 2001.
(6) Pawliszak, J.; Manczyk, K. *Zesz. Nauk. Politech. Slask., Chem.* **1999**, *140*, 199.
(7) Nabuurs, T.; Baijards, R. A.; German, A. L. *Prog. Org. Coat.* **1996**, *27*, 163.
(8) Kulikova, O. A.; Indeikin, E. A.; Manerov, V. B.; Skopintseva, N. B. *Eur. Coat. J.* **2000**, 32.
(9) Kulikova, O. A.; Indeikin, E. A.; Manerov, V. B. *Eur. Coat. J.* **1999**, 44.
(10) Gooch, J. W.; Wang, S. T.; Schork, F. J.; Poehlein, G. W. *Proc. Int. Waterborne, High-Solids, Powder Coat. Symp.* **1997**, *24*, 366.
(11) Dong, H.; Gooch, J. W.; Poehlein, G. W.; Wang, S. T.; Wu, X.; Schork, F. J. *ACS Symp. Ser.* **2001**, *766*, 8.
(12) Abdel-Mohsen, F. F.; Abdel-Hamed El-Zayat, S. *Surf. Coat. Int.* **1992**, *75*, 349.
(13) Jowkar-Deriss, M.; Karlsson, O. J.; Maurer, F. H. J. *J. Appl. Polym. Sci.*, to be submitted.
(14) Jowkar-Deriss, M.; Karlsson, O. J. *Colloids Surf. A: Physicochem. Eng. Aspects*, submitted.
(15) Jowkar-Deriss, M.; Karlsson, O. J. *Polymer*, to be submitted.
(16) Kardos, J. L.; Raisoni, J.; Piccarolo, S.; Halpin, J. C. *Polym. Eng. Sci.* **1979**, *19*, 1000.
(17) Kolarik, J. *Polym. Eng. Sci.* **1996**, *36*, 2518.
(18) Takayanagi, M.; Imida, K.; Kajiyama, T. *J. Polym. Sci., Part C: Polym. Symp.* **1966**, *15*, 263.
(19) Voigt, V. *Lehrbuch der Kristallphysik*; Teuber: Berlin, 1910.
(20) Reuss, A. *Z. Ang. Math. Mech.* **1929**, *9*, 49.
(21) Hashin, Z.; Shtrickman, S. *J. Mech. Phys. Solids* **1963**, *11*, 127.
(22) Hill, R. *J. Mech. Phys. Solids* **1965**, *13*, 213.
(23) Budiansky, B. *J. Mech. Phys. Solids* **1965**, *13*, 223.
(24) Davies, W. E. A. *J. Phys. D: Appl. Phys.* **1971**, *4*, 1325.
(25) Davies, W. E. A. *J. Phys. D: Appl. Phys.* **1971**, *4*, 1176.
(26) Christensen, R. M.; Lo, K. H. *J. Mech. Phys. Solids* **1979**, *27*, 315.
(27) Herve, E.; Zaoui, A. *Int. J. Eng. Sci.* **1993**, *31*, 1.
(28) Maurer, F. H. J. In *Polymer Composites*; Sedlacek, B., Ed.; W. de Gruyter & Co: Berlin, 1986; p 399.
(29) Eklind, H.; Maurer, F. H. J. *Polym. Networks Blends* **1995**, *5*, 35.
(30) Eklind, H.; Maurer, F. H. J. *Polymer* **1996**, *37*, 2641.
(31) Eklind, H.; Maurer, F. H. J. *J. Polym. Sci., Part B: Polym. Phys.* **1996**, *34*, 1569.
(32) Eklind, H.; Schantz, S.; Maurer, F. H. J.; Jannasch, P.; Wesslen, B. *Macromolecules* **1996**, *29*, 984.
(33) Hammer C. O.; Maurer, F. H. J. *Polymer* **1998**, *39*, 4243.
(34) Colombini, D.; Merle, G.; Alberola, N. D. *J. Macromol. Sci., Phys.* **1999**, *B38*, 957.
(35) Colombini, D.; Merle, G.; Alberola, N. D. *J. Appl. Polym. Sci.* **2000**, *76*, 530.
(36) Colombini, D.; Merle, G.; Alberola, N. D. *Macromolecules* **2001**, *34*, 5916.
(37) Colombini, D.; Merle, G.; Alberola, N. D. *Macromol. Symp.* **2001**, *169*, 237.
(38) Ouali, N.; Cavaille, J. Y.; Perez, J. *J. Plast. Rubber Compos. Process. Appl.* **1991**, *16*, 55.
(39) Mele, P.; Alberola, N. D. *Compos. Sci. Technol.* **1996**, *56*, 849.
(40) Colombini, D.; Maurer, F. H. J. *Macromolecules* **2002**, *35*, 5891.
(41) Dickie, R. A. *J. Appl. Polym. Sci.* **1973**, *17*, 45.
(42) Maurer, F. H. J. In *Controlled Interphases in Composite Materials*; Ishida, H., Ed.; Elsevier Science Publishing Co.: New York, 1990; p 491.
(43) Van der Poel, C. *Rheol. Acta* **1958**, *1*, 189.
(44) Fröhlich, J.; Sack, R. *Proc. R. Soc. London* **1946**, *A165*, 415.
(45) Bohn, L. In *Copolymers, Polyblends and Composites: A Symposium*; Platzer, N. A. J., Ed.; American Chemical Society: Washington, DC, 1974; Vol. 6, p 66.

MA030395H